Supporting Information

Hydroxyl-Functional Group Activate Strong Metal-Support Interaction Enabling Efficient Oxygen Reduction Reaction in Saline Water

Xihan Wang [a], Rui Zhang [a,c], Xu Liu [a,c], Yuxin Liu [a,c], Yuxin Zhang [a,c], Guiru Sun [a], Haiyan Wang [a], Junfeng Qin [b], Jingqi Chi [a*], Xiaobin Liu [a,c*], Lei Wang [a*]

a Key Laboratory of Eco-chemical Engineering, International Science and Technology Cooperation Base of Eco-chemical Engineering and Green Manufacturing, College of Chemistry and Molecular Engineering, Qingdao University of Science and Technology, Qingdao 266042, PR China

b Hunan Provincial Key Laboratory of Water Treatment Functional Materials, College of Chemistry and Materials Engineering, Hunan University of Arts and Science, Changde 415000, Hunan, People's Republic of China

c College of Environment and Safety Engineering, Qingdao University of Science and Technology, Qingdao 266042, PR China

* Corresponding authors.

E-mail addresses: chijingqi@qust.edu.cn (J. Chi), liuxb@qust.edu.cn (X. Liu), inorchemwl@qust.edu.cn (L. Wang).

Experimental Section

Materials

Multi-walled carbon nanotubes (MWCNTs) and hydroxylated multi-walled carbon nanotubes (OH-MWCNTs) were purchased from Suiheng Company. Platinum acetylacetonate ($Pt(acac)_2$, 97%), polyvinyl alcohol (PVA), and potassium hydroxide (KOH, 85.0%) were purchased from Aladdin Industrial Corporation. Potassium hydroxide (KOH, 85.0%) was also purchased from Sinopharm Chemical Reagent Co., Ltd. Ethanol (C_2H_6O, 99.7%) and isopropanol (C_3H_8O, 99.7%) were purchased from Shanghai D&B Biotechnology Co., Ltd. Commercial platinum (20% Pt/C) was purchased from Alfa Aesar. Nafion solution (5 wt.%) was purchased from Sigma-Aldrich. Seawater was collected from the Shilaoren Beach in Qingdao. All chemicals were used without further purification. The electrolyte solution was prepared using deionized water (resistivity: 18.2 MΩ).

Synthesis of Pt-CNTs-OH

2 mg of platinum acetylacetonate ($Pt(acac)_2$, 97%) and 10 mg of hydroxylated multi-walled carbon nanotubes (CNTs-OH) were added into a mortar and ground thoroughly for 10 minutes to yield a homogeneous mixture. Subsequently, the resultant mixture was transferred to a 700 W microwave oven and irradiated for 30 seconds.

Synthesis of Pt-CNTs

2 mg of platinum acetylacetonate ($Pt(acac)_2$, 97% purity) and 10 mg of multi-walled carbon nanotubes (CNTs) were added into a mortar and ground thoroughly for 10 minutes to yield a homogeneous mixture. Subsequently, the resultant mixture was transferred to a 700 W microwave oven and irradiated for 30 seconds.

Characterization

The morphological and dimensional characteristics of the samples were characterized using a Hitachi S-8200 Scanning Electron Microscope (SEM) and a JEM-2100UHR Transmission Electron Microscope (TEM) operating at 200 kV. Powder X-ray diffraction (XRD) measurements were performed under Cu Kα radiation with a voltage of 40 kV and a current of 40 mA. The obtained diffraction patterns were subjected to phase analysis and data comparison using MDI Jade software. X-ray photoelectron spectroscopy (XPS) was conducted with a monochromatic Al Kα source (15 mA, 14 kV) to analyze the surface elemental valence states. The content of metal elements in the samples was determined quantitatively using a Varian 710-ES Inductively Coupled Plasma Atomic Emission Spectrometer (ICP-AES).

Electrochemical ORR Measurements

All electrochemical measurements were performed using a three-electrode system at room temperature, with a CHI 760E electrochemical workstation equipped with a glassy carbon ring-disk electrode (RDE) or rotating ring-disk electrode manufactured by PINE Research Instrumentation. The preparation procedure of the catalyst ink was as follows: 5 mg of catalyst was dispersed in 1 mL of mixed solution (containing 700 μL isopropanol, 260 μL deionized water, and 40 μL Nafion solution) and homogenously dispersed via ultrasonic treatment for 1 hour. An appropriate amount of the ultrasonicated catalyst suspension was uniformly coated onto the surface of a glassy carbon working electrode (geometric area: 0.196 cm^2). In the measurement system, the reference electrode was an Ag/AgCl electrode, and the counter electrode was a carbon rod electrode. All measured potentials were converted to reversible hydrogen electrode (RHE) potentials using the following conversion formula: Potential (V vs. RHE) = Potential (V vs. Ag/AgCl) + 0.197 V + 0.0591×pH (1)

Among them, the pH value of the 0.1 M KOH solution was calculated as 13, while the pH value of the mixed solution of 0.1 M KOH and seawater was calculated as 12.8. This is because calcium and magnesium ions in seawater form precipitates with hydroxide ions, resulting in a slight decrease in the pH value of the system. Cyclic Voltammetry (CV) measurements were conducted in O_2-saturated or N_2-saturated 0.1

M KOH solution at a scan rate of 100 mV s^{-1}. RDE measurements for the oxygen reduction reaction (ORR) were carried out in 0.1 M KOH solution, 0.1 M KOH + seawater mixed solution, and simulated seawater solution, respectively, under the conditions of a rotation speed of 1600 rpm and a scan rate of 10 mV s^{-1}.

Oxygen Reduction Reaction Kinetics

The kinetic parameters of the oxygen reduction reaction were determined using the Koutecky-Levich (K-L) equation. The specific method is as follows: Linear Sweep Voltammetry (LSV) was used to scan at different rotation rates, and the current data at different potentials were analyzed to obtain the slope of the best-fit line, which was then used to calculate the Koutecky-Levich curves.

$$\frac{1}{J} = \frac{1}{J_L} + \frac{1}{J_K} = \frac{1}{B\omega^{0.5}} + \frac{1}{J_K} \quad (2)$$

$$J_k = nFkC_0 \quad (3)$$

$$B = 0.62nF(D_0)^{2/3}v^{-1/6}C_0 \quad (4)$$

Among these parameters, J refers to the measured current density, J_K denotes the kinetic term of current density, and J_L represents the limiting diffusion current density. The electrode rotation rate (ω) is expressed in revolutions per minute (rpm). The electron transfer number (n) and peroxide yield (H_2O_2%) were calculated using the following equations:

$$H_2O_2\% = \frac{2I_R/N}{I_D + I_R/N} \times 100 \quad (5)$$

$$n = \frac{4I_D}{I_D + I_R/N} \quad (6)$$

Where I_D and I_R represent the disk current and ring current, respectively. N is the current collection efficiency of the platinum ring (0.37).

The value of electrochemical double-layer capacitance (C_{dl}) was determined from cyclic voltammetry curves obtained at different scan rates in the non-Faradaic region, and its calculation formula is:

$$C_d = \frac{j_a - j_c}{2 \times v} \quad (7)$$

Where j_a and j_c refer to the anodic and cathodic current densities, respectively, which were recorded at the midpoint of the selected potential range (1.15 V vs. RHE); v represents the scan rate.

The stability test was conducted under the aforementioned saturated solution conditions at a rotation speed of 1600 rpm, with a test duration of more than 36000 seconds.

Battery Tests

The open-circuit voltage (OCV) and polarization curve tests of ZABs were performed on a CHI 760E electrochemical workstation. Its discharge performance and cycle stability tests were conducted using a Land CT2001A battery testing system under a current density of 10 mA cm^{-2}.

Aqueous Zinc-Air Batteries

In the zinc-air battery system, the air cathode uses nickel foam as the supporting framework, and its structure is compositely wrapped by a waterproof and breathable membrane and a catalyst layer. The anode adopts a polished zinc sheet, and the electrolyte is a mixed solution of 0.2 M $Zn(OAc)_2$, 6.0 M KOH, and seawater. In addition, a mixed solution of 0.2 M $Zn(OAc)_2$ + 6.0 M KOH + 0.5 M NaCl was selected as the simulated seawater-based electrolyte in the experiment.

Seawater-Based Zinc-Air Batteries

In the seawater-based zinc-air battery, the air cathode uses nickel foam as the supporting substrate, with a waterproof and breathable membrane and a catalyst layer covering its two sides, respectively. The anode uses a polished zinc sheet, and the electrolyte is natural seawater collected from the Shilaoren Beach in Qingdao (pH=8.0).

Flexible Zinc-Air Batteries

In the assembly of flexible alkaline seawater-based zinc-air batteries, the air cathode used a waterproof and breathable membrane loaded with catalyst (isopropanol mixed coating, loading amount: 0.5 mg cm^{-2}), with nickel foam as the supporting substrate. The anode was a polished flexible zinc sheet with a thickness of 3 mm. The air cathode and zinc sheet were placed on both sides of the gel electrolyte, respectively, and

encapsulated with a thermoplastic film. The preparation process of the gel electrolyte was as follows: 2 g of polyvinyl alcohol (PVA) was added to 16 mL of seawater, heated and dissolved at 90°C. Then, 4 mL of 9.0 M potassium hydroxide-seawater mixed solution was added, and heating and stirring were continued for 20 minutes. After the system was cooled to room temperature, it was frozen for 3 hours, and finally stored in a refrigerator for later use.

Computational details

All calculations were performed using the density functional theory (DFT) technique using the Vienna ab initio simulation package (VASP).[1] Spin-polarized calculations were performed using the generalized gradient approximation (GGA) combined with the Perdew–Burke–Ernzerhof (PBE) method to determine the exchange and correlation energies. The projector-augmented wave (PAW) method was used to represent the core–valence electron interactions. For geometry optimization calculations, forces were converged below 0.03 eV/Å. The SCF convergence energy was 1×10^{-4} eV. A 1 × 1 × 1 k-point mesh was used to perform all the calculations.

One layer graphene structure was constructed to simulate CNT substitution for calculating the adsorption energies and Gibbs free energies. According to the results of XPS, the edges of graphene are connected with different numbers of OH groups. Six Pt atoms were placed on the surface of graphene to simulate Pt clusters for building Pt-CNTs and Pt-CNTs-OH samples. A vacuum of 15 Å was used to simulate the surface under periodic boundary conditions.

The adsorption energy (E_{ads}) of the O_2 and the other molecule on the surface was calculated as follows (eq 8):

$$E_{ads} = E_{adsorbate + surface} - E_{surface} - E_{gas}, \quad (8)$$

The ORR estimation follows four elementary steps. The free energies of the intermediates at 298.15 K were obtained by:

$$\Delta G=\Delta E+\Delta E_{ZPE}-T\Delta S-eU \quad (9)$$

where ΔS and U are the zero-point energy changes, entropy changes, and applied potentials. ΔE is the binding energy of adsorption species HO*, O*, and HOO*, with defined as follows:

$$\Delta E =E_{substrate+adsorbate}-E_{substrate}-E_{adsorbate} \quad (10)$$

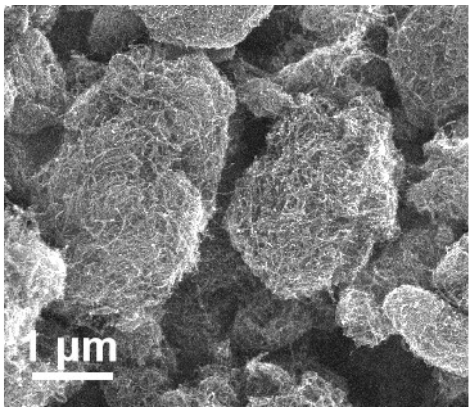

Figure S1. SEM image of Pt-CNTs-OH.

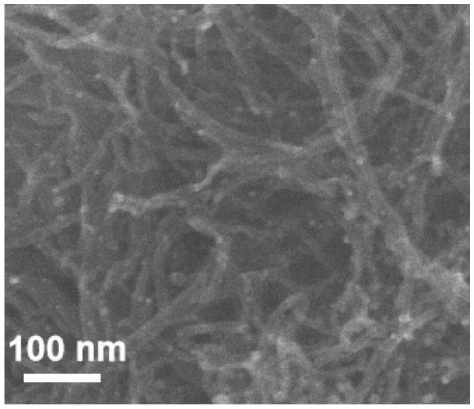

Figure S2. SEM image of Pt-CNTs.

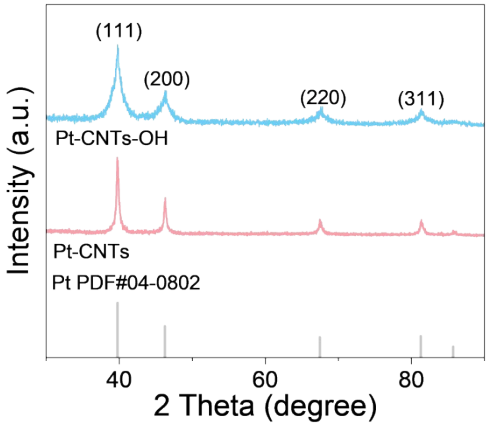

Figure S3. XRD patterns of Pt-CNTs-OH and Pt-CNTs.

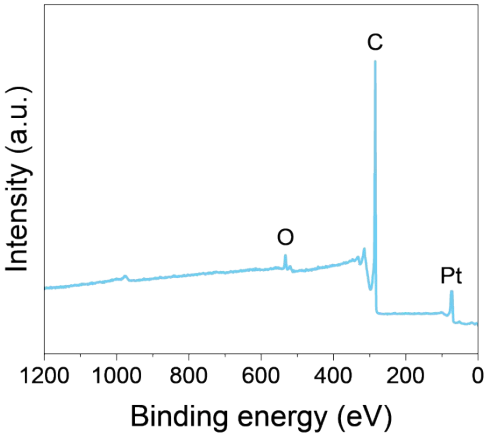

Figure S4. XPS survey spectrum of Pt-CNTs-OH.

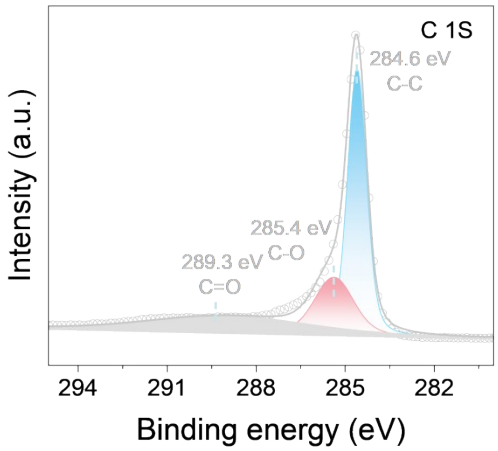

Figure S5. C 1s spectrum of Pt-CNTs-OH.

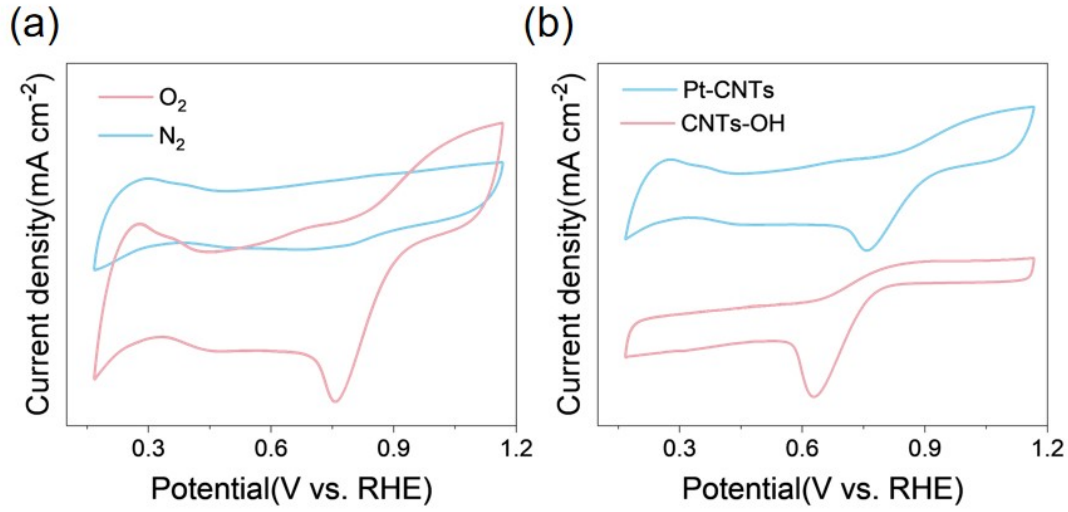

Figure S6. Electrochemical performances. (a) Cyclic voltammograms of Pt-CNTs-OH in 0.1 M KOH saturated with O_2 and N_2. (b) Cyclic voltammograms of Pt-CNTs and CNTs-OH in O_2-saturated 0.1 M KOH.

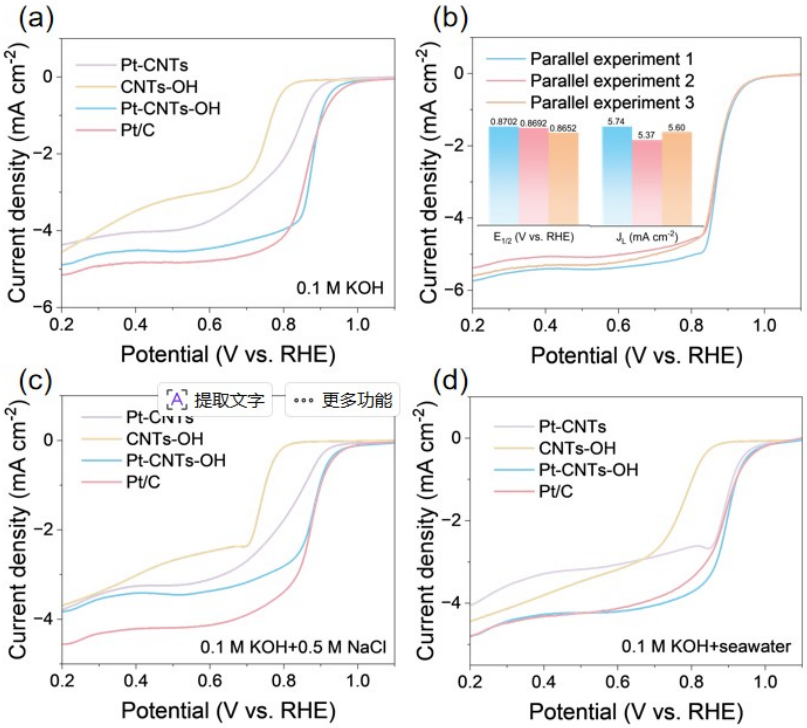

Figure S7. (a) ORR polarization curves in 0.1 M KOH. (b) ORR LSV curves of Pt-CNTs-OH synthesized from three parallel experiments in 0.1 M KOH at 1600 rpm (inset: comparison of $E_{1/2}$ and J_L values). (c) ORR polarization curves in 0.1 M KOH and 0.5 M NaCl. (d) ORR polarization curves in 0.1 M KOH with seawater.

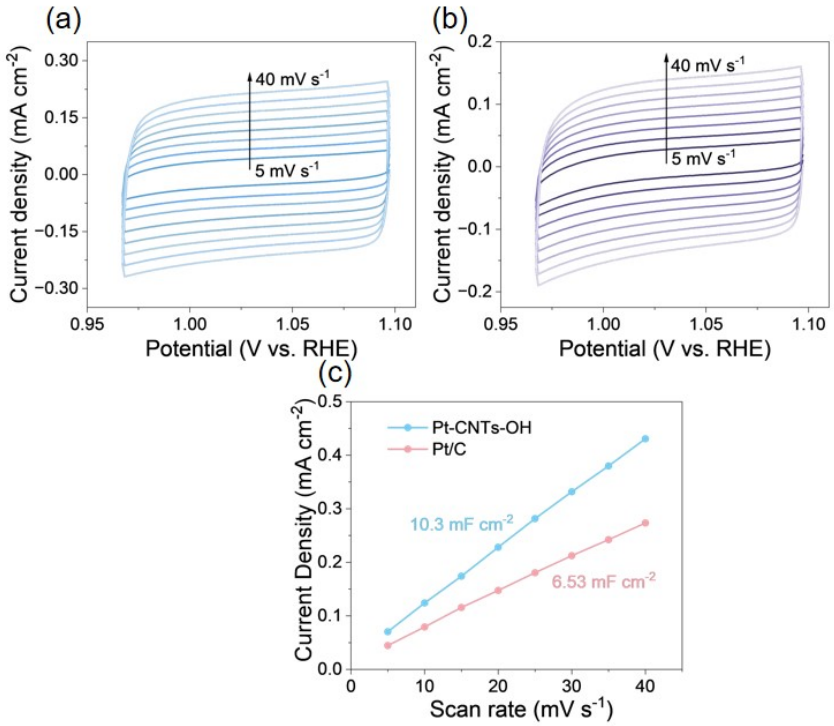

Figure S8. CV measurements of (a) Pt-CNTs-OH and (b) Pt/C at different scan rates, respectively, in 0.1 M KOH. (c) C_{dl} of Pt-CNTs-OH and Pt/C in 0.1 M KOH.

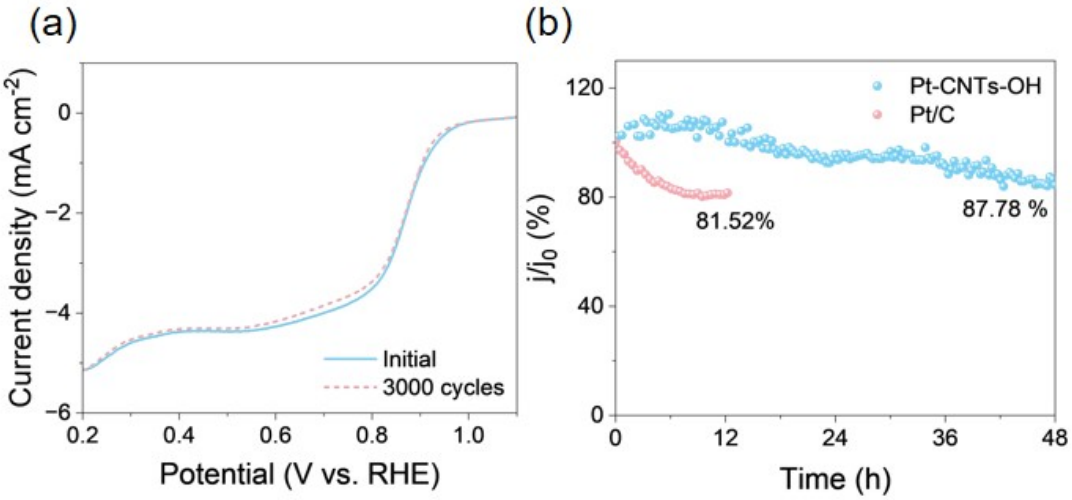

Figure S9. (a) 3000 cycles of Pt-CNTs-OH. (b) I-t test in 1.0 M KOH.

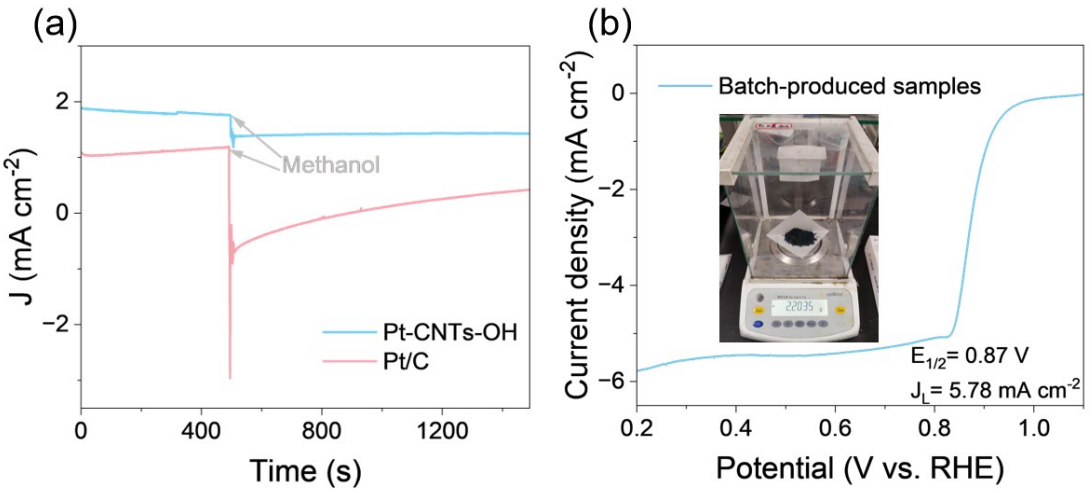

Figure S10. (a) Methanol tolerance tests of Pt-CNTs-OH and Pt/C. (b) ORR LSV curve of batch-produced Pt-CNTs-OH catalyst in 0.1 M KOH at 1600 rpm. Inset: photograph of the batch-prepared Pt-CNTs-OH catalyst.

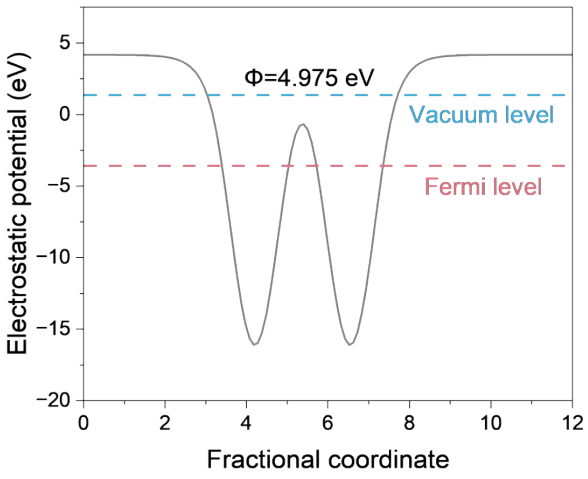

Figure S11. Work function of Pt-CNTs.

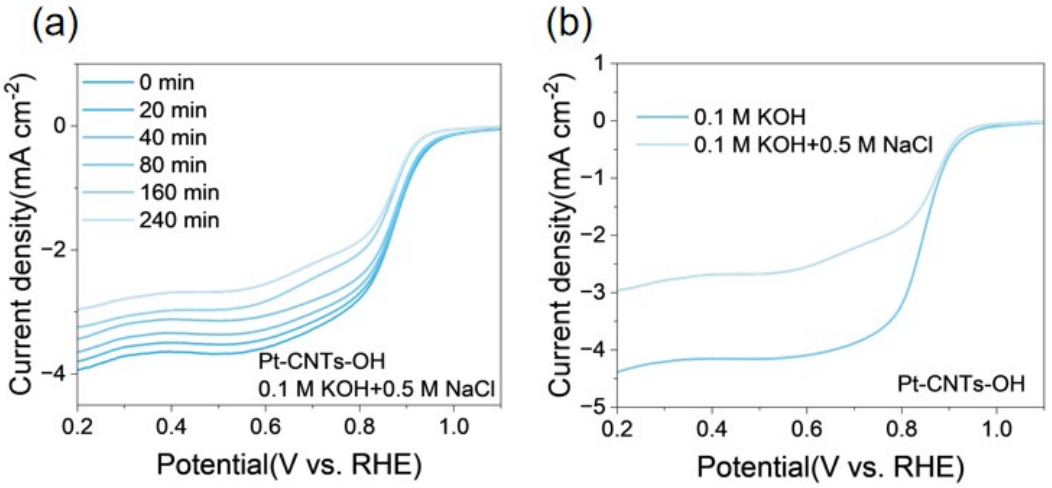

Figure S12. (a) LSV curves of Pt-CNTs-OH tested at different time intervals in 0.1 M KOH + 0.5 M NaCl. (b) Performance of Pt-CNTs-OH subsequently tested in 0.1 M KOH, after being immersed in 0.1 M KOH and 0.1 M KOH + 0.5 M NaCl for 240 min respectively.

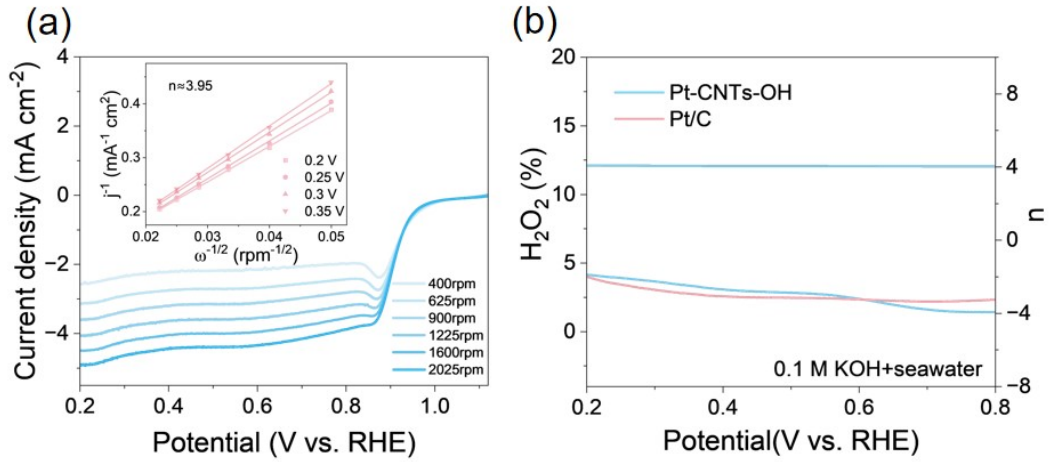

Figure S13. (a) ORR polarization curves at different rotation speeds in 0.1 M KOH + seawater (inset: fitted plots of the K-L equation at different voltages). (b) Peroxides and electron transfer numbers obtained in 0.1 M KOH + seawater.

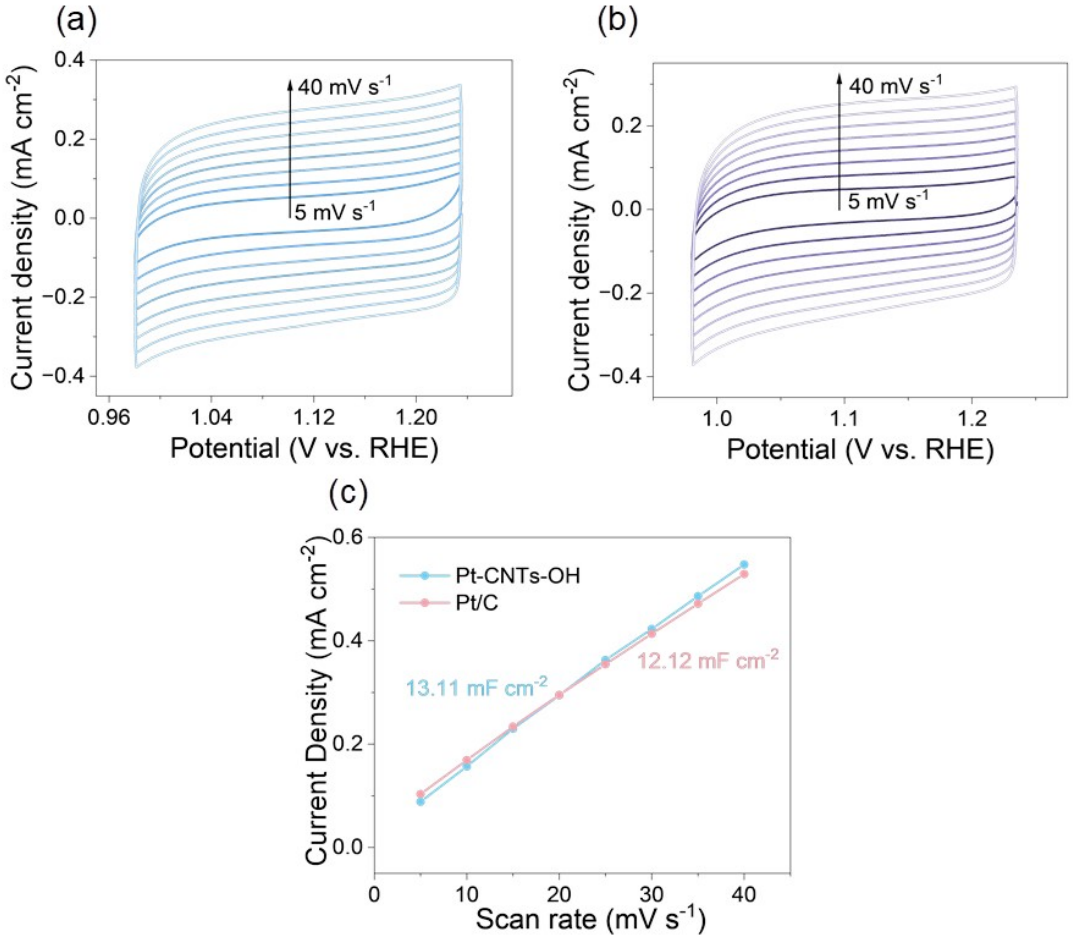

Figure S14. CV measurements of (a) Pt-CNTs-OH and (b) Pt/C at different scan rates, respectively, in 0.1 M KOH + seawater. (c) C_{dl} of Pt-CNTs-OH and Pt/C in 0.1 M KOH + seawater.

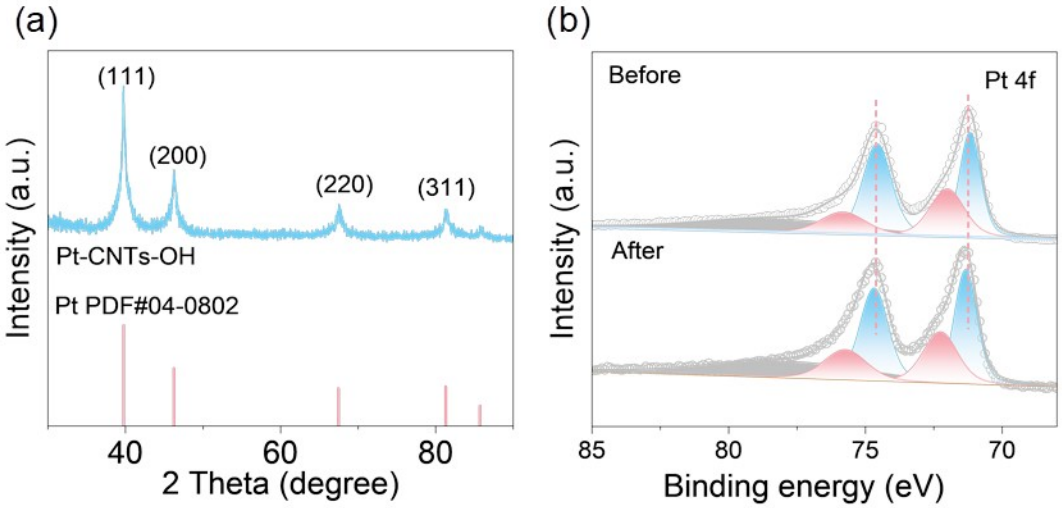

Figure S15. Material characterization of Pt-CNTs-OH after ORR stability test. (a) XRD patterns. (b) Pt 4f XPS spectrum.

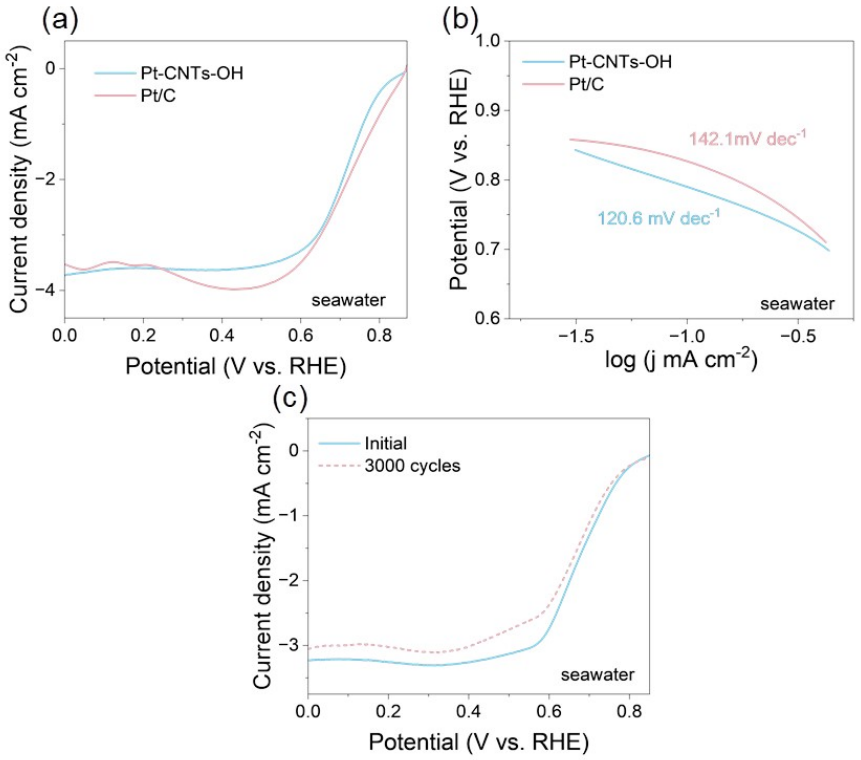

Figure S16. (a) LSV curves for the ORR of Pt-CNTs-OH and Pt/C in natural seawater at 1600 rpm. (b) Corresponding Tafel slopes of Pt-CNTs-OH and Pt/C in natural seawater. (c) ORR durability test in natural seawater.

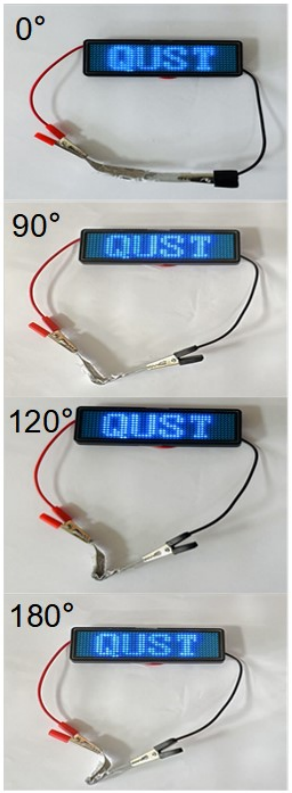

Figure S17. Photos of LEDs powered by a flexible ZAB at different bending angles.

Table S1. Characterization of the mass ratio of Pt in Pt-CNTs-OH and Pt-CNTs via ICP-AES.

Samples	Elements	Mass ratios (%)
Pt-CNTs-OH	Pt	10.64
Pt-CNTs	Pt	10.70

Table S2. Comparison of ORR performance with some reported electrocatalysts under alkaline conditions (0.1 M KOH).

Materials	**E_{onset} (V) (V vs. RHE)**	**$E_{1/2}$ (V) (V vs. RHE)**	**Tafel slope (mV dec^{-1})**	**n**	**H_2O_2 (%)**	**Ref.**
Pt-CNTs-OH	**0.97**	**0.8732**	**79.5**	**3.94**	< 3.5%	**This work**
PhFCC-400	0.94	0.85	--	3.94	< 2.3%	[2]
Fe-CN_x/CNTs	0.95	0.82	--	3.96	< 7.5%	[3]
Mn/Co-C-N	0.89	0.8	60	3.995	--	[4]
Cu,S,N-C	0.945	0.847	--	--	--	[5]
Fe_3Mn_1-NrGO	0.96	0.84	70.3	3.9	< 1%	[6]
Fe_2P/NPC	0.997	0.872	86	3.95	< 2.4%	[7]
TEPT-TA-800	0.94	0.85	59.1	3.8	11%	[8]
FePc@CNF	0.966	0.875	43.1	3.8	3.82%	[9]
PMS-CNT/C-b	0.99	0.77	--	3.76-3.93	--	[10]
Fe_3O_4/N-CNTs-2	0.92	0.804	--	--	< 10%	[11]

Table S3. Comparison of Zinc-air battery performance with some reported transition metal electrocatalysts.

Materials	Open-circuit potential (V)	Specific capacity (mAh g^{-1})	Power density (mW cm^{-2})	ZAB stability (h)	Ref.
Pt-CNTs-OH	**1.437**	**810.8**	**166**	**855**	**This work**
CoP/Co_2P-6@NC/MWCNTs	1.49	805.26	134.36	500	[12]
ZnS@C-2	1.49	836	120.4	165	[13]
Co_4N/PNC-920	1.462	801.1	170.7	270	[14]
CoFe-FeNC	1.447	767.5	120.8	1200	[15]

References

1. C. Feng, G. Xiong, C. Chen, Y. Lin, Z. Wang, Y. Lu, F. Liu, X. Li, Y. Liu, R. Zhang and Y. Pan, *Chin. J. Catal.*, 2025, **75**, 21-33.
2. S. Samireddi, V. Aishwarya, I. Shown, S. Muthusamy, S. M. Unni, K. T. Wong, K. H. Chen and L. C. Chen, *Small*, 2021, **17**, 2103823.
3. C. Xiao, X. Chen and Y. Tang, *Nanotechnology*, 2017, **28**, 225401.
4. Y. Qiao, Y. Guo, Y. Zhao, C. Chang, S. Wang, X. Zhang, F. Gao, R. Chen and L. Hou, *Nanotechnology*, 2024, **36**, 035703.
5. Y. Zhao, Y. Yu, Y. Wang, J. Ma and S. Xing, *Catal. Lett.*, 2021, **152**, 2342-2351.
6. K. Bhunia, J. H. Seok, M. Perumalsamy, K. S. Bejigo, V. Elumalai, S. U. Lee and S.-j. Kim, *Nano Energy*, 2024, **129**, 109966.
7. L. Chen, Y. Zhang, L. Dong, X. Liu, L. Long, S. Wang, C. Liu, S. Dong and J. Jia, *Carbon*, 2020, **158**, 885-892.
8. L. Liu, Z. Xu, Y. Xia, M.-Y. Gao, Q. Jin, B. Zheng, C. Liu, S. Chen, Z. Zhang and H.-L. Wang, *Chem. Eng. J.*, 2024, **497**, 155560.
9. Y. Wu, J. Liu, Q. Sun, J. Chen, X. Zhu, R. Abazari and J. Qian, *Chem. Eng. J.*, 2024, **483**, 149243.
10. B. Zhang, R. Chen, Z. Yang, Y. Chen, L. Zhou and Y. Yuan, *Int. J. Hydrogen Energy*, 2019, **44**, 31094-31103.
11. K. Song, J. Wei, W. Dong, Z. Zou and J. Wang, *Int. J. Hydrogen Energy*, 2022, **47**, 20529-20539.
12. X. Cui, X. Li, M. Hu, W. Teng, L. Zong, Y. Dan and L. Chen, *J. Electroanal. Chem.*, 2025, **979**, 118919.
13. C. Lin, Y. Yin, G. Wang, X. Cao and J. Ma, *Int. J. Hydrogen Energy*, 2024, **93**, 221-228.
14. B. Li, Y. Ren, G. Zhang, C. Lv, L. Li, X. Yang, Z. Lu, X. Zhang and X. Yu, *Appl. Surf. Sci.*, 2025, **679**, 161212.
15. S. Zhang, J. Yang, L. Yang, T. Yang, Y. Liu, L. Zhou, Z. Xu, X. Zhou and J. Tang, *Appl. Catal. B Environ. Energy*, 2024, **359**, 124485.